Available online at www.sciencedirect.com

jmr&t Journal of Materials Research and Technology

www.jmrt.com.br

Original Article

Mechanical and wear behaviour of poly(vinylidene fluoride)/clay nanocomposite

Anupama Gaur[a], *Dipak Rana*[b], *Pralay Maiti*[a,*]

[a] *School of Materials Science and Technology, Indian Institute of Technology (Banaras Hindu University), Varanasi 221005, India*

[b] *Industrial Membrane Research Institute, Department of Chemical and Biological Engineering, University of Ottawa, 161 Louis Pasteur St., Ottawa, ON KIN 6N5, Canada*

ARTICLE INFO

Article history:
Received 5 January 2019
Accepted 20 September 2019
Available online 19 October 2019

Keywords:
PVDF
Wear
Hardness
Morphology

ABSTRACT

Poly(vinylidene fluoride) (PVDF)/organically modified nanoclay composites using different amount of nanoclay have been prepared through solution route. The structural changes are determined through X-ray diffraction and Fourier transform infrared spectroscopy studies, which show the transformation from α to β-phase crystallization in presence of nanoclay. Polarised optical microscopic images show the changes of spherulite pattern into mesh like pattern in presence of nanoclay. Modulus of PVDF-nanocomposite increase with increasing the nanoclay content up to 4 wt.% and then slightly decreases under uniaxial tension and the improvement in mechanical responses are fitted with theoretical models. Tribological behaviour of PVDF nanocomposites is evaluated and found that nanoclay content upto 4 wt.% is effective in decreasing the wear and coefficient of friction of PVDF. Similarly, hardness of the nanocomposites also increases for clay content upto 4 wt.%. The nanoclay is working as reinforcing agent for PVDF and is improving its mechanical and frictional properties.

1. Introduction

Polymer composites have potential applications in mechanical engineering as frictional and structural materials. They have low density, easy processability along with strength, good thermal stability and wear resistance. These properties make polymer composites important for tribological-applications and are used in diverse field such as aerospace, automobile industry, biomechanics and electronic industry. Incorporation of nanoparticles in the polymer is an interesting method for polymer modification as it produces materials with variable properties, which can be used in different fields. In past years many composite materials having inorganic or organic fillers, have been prepared, which has potentially increased the application of polymeric materials [1]. For example, the addition of fillers like reinforcing fibers and organic/inorganic fillers effectively improves the tribological properties of the polymers [2]. Fluoropolymers have excellent chemical and thermal stabilities as compared to hydrocarbon polymers. These qualities make them appropriate for applications where thermal stability, chemical resistance, low acoustic impedance, mechanical stability and wear resistance is required. Poly(vinylidene fluoride) (PVDF) is an important fluoropolymer known for its excellent solvent resistance, UV

* *Corresponding author.*
E-mail: pmaiti.mst@itbhu.ac.in (P. Maiti).

https://doi.org/10.1016/j.jmrt.2019.09.059

exposition, inflammable, thermal oxidative degradation and hydrolytic stability [3,4]. PVDF is used in diverse fields such as paper and pulp industry, chemical processing industry and high temperature applications [5]. It is also used in electromechanical and electroacoustic transducers because of its piezoelectric [6] and pyroelectric [7] properties. PVDF is also used as ferroelectric polymer [4], a membrane material for water filtration [8] and as a separator, binder and electrolyte in rechargeable lithium batteries [9], in sensors [10]. PVDF is semicrystalline polymer with four phases α, β, γ and δ, which are formed according to processing conditions [11]. Most common phases studied are the nonpolar α-phase and polar β and γ-phase [12]. The β-phase shows piezoelectric, ferroelectric, dielectric and high permittivity [13]. Filler material is incorporated to improve the functional properties, structure and morphology of PVDF. Ionic substances like, hydrated salts [14], ionic liquids [15], organically modified silicates (OMS) [16,17] helps in inducing the ferroelectric β-phase of PVDF [18]. Carbon black [19] and carbon nanotubes [20] were blended with PVDF to obtain electrically conducting composites. Two dimensional materials like graphene and graphene oxide induce variety of functional properties in PVDF like inducing piezoelectric phase, electrical and thermal conductivity, improving dielectric constant and the formation of hydrophilic and super hydrophobic surfaces. Different techniques like melt crystallization at high pressure [21], high voltage poling [22] and mechanical processing [23] are also used for inducing the electroactive β-phase. OMS also shows dramatic enhancement in mechanical properties [24].

Fillers like, graphene oxide [25], carbon black [26], carbon fiber [27] and nanoclay [5] have been used to improve the tribolocal properties of PVDF. The tribological properties of blend prepared by PVDF and ultrahigh molecular weight polyethylene (UMHWPE) (70/30) is studied by Brostow et al. [26], in which the polyethylene was γ-irradiated or un-irradiated and each blend sample contain different amount of carbon black. It is found that for an optimized carbon black concentration and a specific irradiation dose, the wear reduces with high scratch resistance and lower friction. Bismarck and Schulz [27] prepared the PVDF composite by reinforcing fluorinated, polyacrylonitrile-based high strength carbon fiber and found that the friction of composite decreases as they increase the degree of fluorination of fiber. Garcia et al. [28] explained the wear and mechanical properties in PVDF and PMMA blend through phase morphology of the system, as the blend does not follow the simple additive rule. Achaby et al. [29] prepared PVDF/reduced graphene oxide nanocomposite using the melt blending method and found significant improvement in the flexural modulus, tensile modulus, flexural and tensile strength and the thermal stability. Thangavel et al. [25] evaluated the tribological properties of the PVDF/functionalized graphene oxide thin film and found that the composite was stable even after 120 cycles of 10 mN load in reciprocating motion. In the composite technology, the polymer layered silicate nanocomposite is one of the important steps. In order to form ordered nanocoposites [30], the solution casting and melt intercalation technique is used to insert the polymer in the interlayer spacing of the silicate layers. Peng at al. [5]. explained the tribological properties of the PVDF nanoclay composites with different nanoclay content and found that the 2% nanoclay containing composite shows enhanced tribological properties. Priya et al. [31] found that the storage modulus increase dramatically in nanocomposite of PVDF and clay, prepared using the melt intercalation method. It is also reported that the nanoclay helps in improving the tribological properties of polyester [32] and polyamide [33] efficiently. Lai et al. prepared nanocomposite of PVDF and nanoclay with different organic modifiers and found enhanced abrasive resistance and mechanical strength [34].

In this study, the PVDF/nanoclay composites with different nanoclay content were prepared using the solution route. The structure, morphology and thermal properties are studied through X-ray diffraction, Fourier transform infrared spectroscopy, scanning electron microscopy, atomic force microscopy, thermo-gravimetric analysis and differential scanning calorimetry. The mechanical and friction properties are investigated using universal testing machine and wear tester. The effect of different nanoclay content on mechanical, thermal and tribological properties has been discussed.

2. Experimental section

2.1. Materials used

Poly(vinylidene fluoride) commercial SOLEF, 6008 with molecular weight 2.7×10^5 was used, which was supplied by Ausimont, Italy. An organically modified clay, Cloisite 30B with density 1.98 g/cc, obtained from Southern Clay Inc., USA. Dimethyl formamide (DMF), purchased from Himedia, India is used as a common solvent/media for both polymer and clay.

2.2. Preparation of nanocomposite

Nanocomposites of poly(vinylidine fluoride) and organically modified nanoclay have been prepared using the solution method. Different concentrations of clay have been used for the preparation of nanocomposites (1, 2, 4, 8 and 10 wt.% of clay with respect to polymer weight). In this method, PVDF is first dissolved in DMF at 60 °C and clay is separately dispersed using sonication method. After this, both the solutions of polymer and nanoclay are mixed together by stirring followed by sonication for proper dispersion. Then solvent removal is done by pouring it into petri dish and kept at 60 °C in vacuum oven dried for overnight. Similarly PVDF is also dissolved in DMF and kept in oven for solvent removal. Pristine PVDF and nanocomposites are abbreviated as P, PC1, PC2, PC4, and PC8 for 0, 1, 2, 4, 8 wt% of nanoclay, respectively.

2.3. Sample preparation

For characterization of the pristine PVDF and nanocomposites, films were prepared through compression moulding techniques. For tensile testing, dog bone shaped samples are prepared using injection moulding technique. For wear testing, specimens of $2 \times 3 \times 12.5\ mm^3$ dimension are prepared.

2.4. Characterization

Transmission electron microscopy (TEM): The distribution of the filler (nanoclay) in PVDF is examined by transmission electron microscope. A PhilipsCM-10 operated at an accelerating voltage of 100 kV was used to take the TEM images. A thin layer of the sample was sectioned at −80 °C by a Leica ultra-cut microtome equipped with a diamond knife. *X-Ray diffraction (XRD):* The exfoliation of nanoparticles and the changes in structure is analysed using XRD analysis. XRD plots of the pristine polymer and its nanocomposite are taken using a Rigaku Miniflex 600 diffractometer, which operates at a voltage of 40 kV and a current of 15 mA using CuKα radiation (λ = 1.54 Å). The d-spacing, distance between clay platelets is calculated using Bragg's formula d = λ/(2 s in.), where, θ is the diffraction angle and λ is the wavelength of X-ray [35]. *Fourier transform infrared spectroscopy (FTIR):* FTIR is performed using Nicolet 5700 at room temperature in the 650 to 4000 cm^{-1} range with 4 cm^{-1} resolution in ATR mode. *Polarized Optical Microscopy (POM):* To examine the structure of PVDF and its nanocomposites, the samples were observed in Leitz Biomed microscope after suitable crystallization. *Scanning electron microscopy (SEM):* PVDF and nanocomposite morphology is investigated using SEM (Zeiss, Supra). Samples of PVDF and its nanocomposites are gold coated before observation in SEM using a sputtering apparatus. *Thermogravimetric analysis (TGA):* Thermal stability of pristine polymer and nanocomposite is studied using TGA. The samples are taken in alumina pans. The samples are heated at a scan rate of 20° min^{-1} upto a temperature of 600 °C. *Differential scanning calorimetry (DSC):* To investigate the melting temperature and crystallinity of pristine PVDF and nanocomposites, DSC experiment is performed using DSC (Mettler Toledo 832), at a heating rate of 10 °C/min. Small amount of samples ($\tilde{2}$ mg) is taken for measurement and platinum pans are used for the measurements. The instrument is calibrated using indium before measurement. *Tensile testing:* Instron Universal Tensile Machine is used to complete the tensile test. The data is collected up to the breaking of the dog bone samples at a strain rate of 5 mm/min. *Wear testing:* Wear testing is performed using Ducom wear tester. The pin on disk type setup is used for the wear measurement. The measurements are taken at different loads using speed of 100 RPM and track diameter of 80 mm. *Vickers hardness test:* Hardness of pristine PVDF and nanocomposites is determined using Tinius Olsen micro hardness tester. Indents at different load are measured and three readings are taken for all measurements to understand the error estimate. *Statistical analysis:* The results of mechanical properties are expressed as mean value. Statistical comparisons are carried out by single factorial analysis of variance (One-way ANOVA with t-test).

3. Results and discussion

3.1. Structure and morphology

The dispersion of nanoclay platelets in PVDF matrix is observed through TEM. Fig. 1a shows the TEM image of 4 wt.% nanocomposite (PC4). Clay platelets are uniformly dispersed in PVDF matrix. The surface modification of nanoclay has increased the interaction between clay and polymer leading to better dispersion in polymer matrix. Structure of pristine PVDF and its nanocomposites are determined throughXRD studies. Fig. 1b shows the XRD patterns for PVDF and its nanocomposites with various nanoclay contents. The characteristic peaks in pristine PVDF occurs at $2\theta\tilde{1}7.5°$ (020), 18.3° (100), 19.9° (110) and 26.7° (021) [25,36], which indicate that the PVDF crystallizes in α-crystalline phase. On the other hand, a new peak at $2\theta\tilde{2}0.3°$ arises corresponding to β-phase in the nanocomposites and simultaneously the intensity of α-phase peak decreases with increasing the nanoclay content. Apparently, β-phase peak increases with clay content in the nanocomposites.

Fig. 1c shows the different phase fractions in the pristine PVDF and nanocomposites, which is calculated through the deconvolution of XRD peaks of the corresponding nanocomposite. The deconvolution pattern of nanocomposite is shown in Supplementary Fig. S1. It is evident that β and γ-phase fraction increases with greater amount of nanoclay while systematic reduction of α-phase occurs in higher clay content nanocomposites. However, XRD analysis shows that the nanoclay is acting as β-nucleating agent, which leads to the alteration from α to β/γ-phase. The decreased intensity of α-phase peak suggests the gradual disappearance of α-phase in presence of nanoclay layers [31]. The polarity of the polymer chain is increasing with increasing the clay content as α-phase is non-polar and β-phase is polar [37]. FTIR spectroscopy is also used to explore the structure of nanocomposites. Fig. 1d shows the FTIR plot of pristine PVDF and its nanocomposites with two representative nanoclay content nanocomposites. FTIR bands at 760, 796 and 996 cm^{-1} correspond to the α-phase, which intensities decrease in the nanocomposites. On the other hand, nanocomposites have new bands at 840 and 880 cm^{-1} that are characteristic for electroactive β-phase [38]. The band at 840 cm^{-1} corresponds to both the β and γ-phase. At higher wavenumber region, a characteristic band at 1232 cm^{-1} for β-phase is also observed in nanocomposite (Supplementary Fig. S2) along with a band at 1272 cm^{-1} assigned for γ-phase. The structural changes are reflected in the change of bulk morphology. Fig. 1e shows the polarized optical microscopic images for pristine PVDF and its nanocomposites. Pristine PVDF shows the spherulitic structure due to presence of α-phase, which diminishes in the nanocomposite and instead mesh like morphology is obtained due to the formation of β-phase [25]. Hence, structural alteration in presence of nanoclay is manifested in bulk morphology.

3.2. Thermal analysis

Fig. 2a shows the DSC thermograms of pristine PVDF and the nanocomposites. The melting temperature of the pristine PVDF is 175 °C, which has increased to 178.2 and 178.5 °C for PC4 and PC8 nanocomposite, respectively. Overall increase of melting temperature in the nanocomposites is due to the presence of γ-phase as it is known that melting point of γ-phase is higher than α-phase while pure β-phase melting is lower

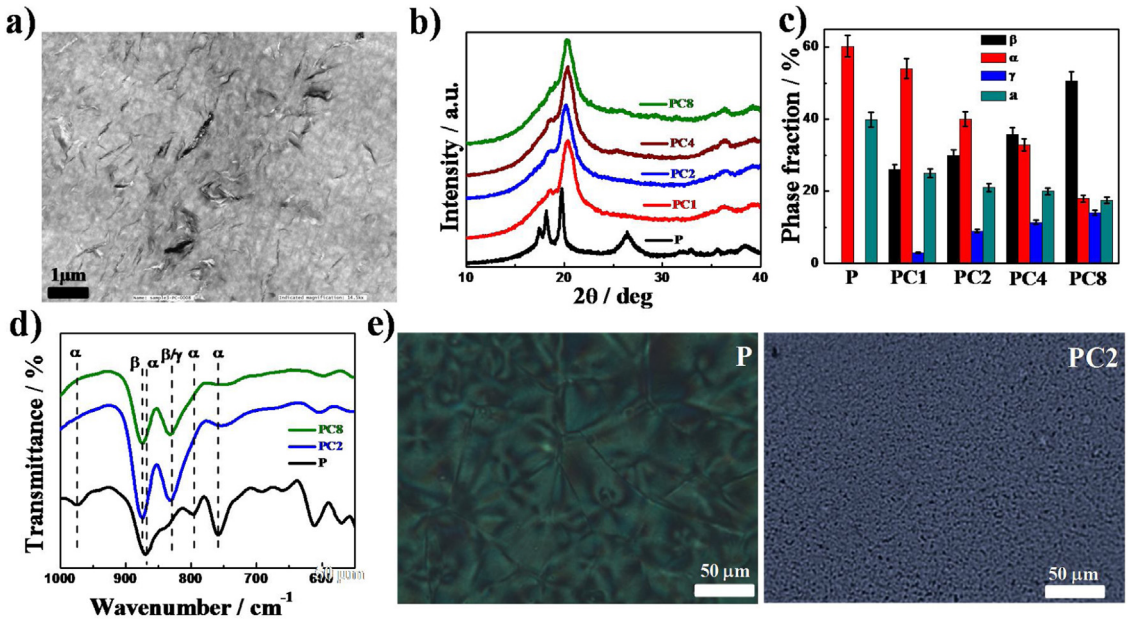

Fig. 1 – (a) TEM image of PC4; (b) X-ray diffraction patterns of indicated nanocomposites; (c) phase fractions of indicated nanocomposites measured through peak deconvolution; (d) FTIR spectra of indicated specimens; and (e) polarized optical microscopic images of pristine PVDF and its nanocomposite (PC2).

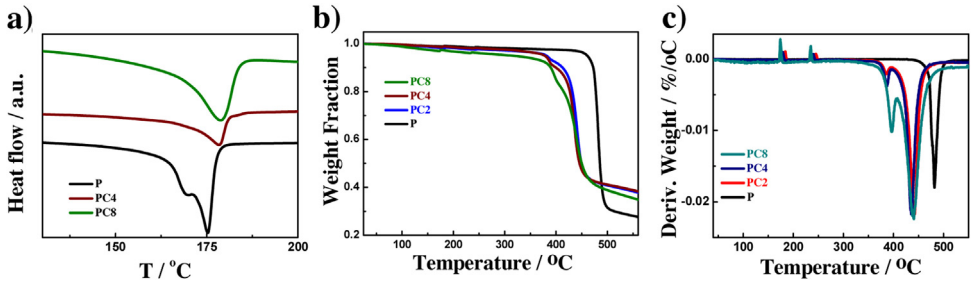

Fig. 2 – (a) DSC curves for pristine PVDF and its nanocomposites; (b) TGA curves showing degradation behaviour of PVDF and indicated nanocomposites; and (c) DTG plots for pristine PVDF and its nanocomposites.

than the α-phase. The crystallinity and the enthalpy of the semi-crystalline polymer are related by:

$$X_c = \frac{\Delta H_m}{\Delta H_m^o} \times 100\,\% \quad (1)$$

where X_c is crystallinity, ΔH_m is the apparent enthalpy of fusion per gram of polymer sample, which is calculated from DSC curve and ΔH_m° is the enthalpy of fusion per gram of 100% crystalline polymer (for PVDF $\Delta H_m^\circ = 105$ J/g) [39]. The calculated crystallinities for P, PC4 and PC8 are 39.35, 37.2 and 34.04 J/g, respectively. The reduction of heat of fusion is lower for β/γ phase as compared to regular α-phase of crystallites. Although the nanoclay induces the β-phase in PVDF, it simultaneously decreases the crystallinity of PVDF to make it flexible and tough. Fig. 2b shows the thermogravimetric curves of mass loss as a function of temperature (TGA graphs) and Fig. 2c shows corresponding differential thermogravimetric plots for pristine PVDF and nanocomposites. The onset temperatures of degradation for P, PC4 and PC8 are decreasing gradually as 461.8, 380.0 and 331.7 °C, respectively, as measured from the temperature corresponding to 5% mass loss. This decrease in degradation temperature is triggered by the presence of nanoclay.

3.3. *Mechanical properties*

The stress-strain curves ofpristine PVDF and the nanocomposites are obtained using uniaxial tensile testing (Fig. 3a). Young's modulus (Fig. 3b) of the nanocomposites increases up to 4 wt.% nanoclay and after that slightly decrease for 8 wt.% nanocomposite but the elongation at break or the toughness (Supplementary Fig. S3) of the nanocomposites increases gradually with the increasing nanoclay. The results reflect that different reinforcement effects can be achieved by the nanoclay dispersion in the PVDF matrix. Low loading (up to 4 wt.%) is effective to improve the mechanical properties of the nanocomposites (30% for modulus using 4 wt.% nanoclay). This can be explained by the enhanced energy dissipation due to the tiny and more mobile β-phase crystals in the nanocomposites [40].

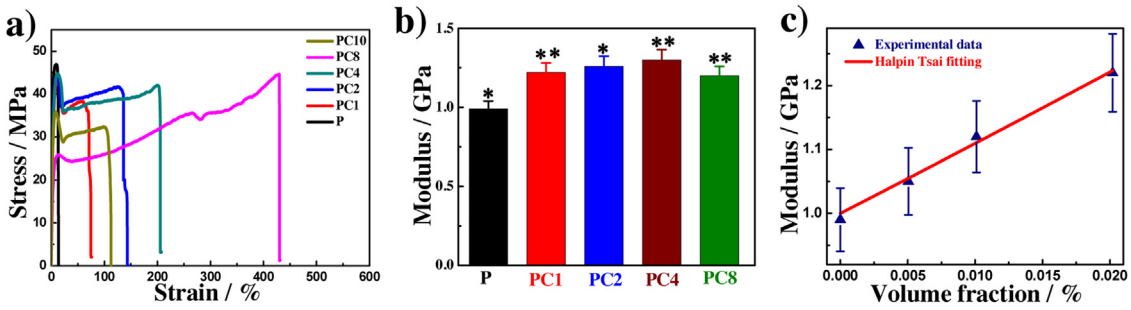

Fig. 3 – (a) Stress–strain curves if indicated specimens; (b) Young's modulus for pristine PVDF and indicated nanocomposites as calculated from the stress–strain curves; the results presented are mean values obtained from three independent experiments, where $^{*}P < 0.05$, $^{**}P < 0.01$ and $^{***}P < 0.0001$; (c) experimental curve fitting of the data points using Halpin–Tsai equation.

Halpin et al. [41] equation is used to calculate the effect of volume fraction of the filler, relative modulus of the components and the reinforced geometry of the composite moduli. The Young's modulus of the nanocomposite is related to these parameters with a mathematical equation [42,43]. If we consider the random distribution of the nanoclay in PVDF matrix in the nanocomposites, the modified form of Halpin and Tsai equation may be written as [44,45]:

$$E_y = \left[\frac{3}{8}\frac{1+(2L_G/3T_G)\eta_L V_G}{1-\eta_L V_G} + \frac{5}{8}\frac{1+2\eta_T V_G}{1-\eta_T V_G}\right] E_P \quad (2)$$

where

$$\eta_L = \frac{(E_G/E_P)-1}{(E_G/E_P)+(2L_G/3T_G)}, \eta_T = \frac{(E_G/E_P)-1}{(E_G/E_P)+2}$$

where E_Y, E_G and E_P are Young's modulus of the composite, nanoclay and polymer, respectively. L_G, T_G and V_G are the length, thickness and volume fraction of the nanoclay in the nanocomposites, respectively. The modified Halpin–Tsai equation for unidirectional/ parallel orientation of the nanoclay layers in the polymer matrix is represented by:

$$E_Y^m = \left[\frac{1+(2L_G/3T_G)\eta_L V_G}{1-\eta_L V_G}\right] \quad (3)$$

As Halpin–Tsai is based on the assumption that the filler is randomly distributed in the matrix, the experimental data fits well with the Haplin–Tsai Eq. (3). From the Fig. 3c, it is clear that the experimental values are almost same as the theoretical curve drawn assuming the unidirectional distribution. The value of aspect ratio from Halpin–Tsai fitting is 10.59, which is very similar to the value obtained (~9.86) from the TEM image. The slight difference between the predicted and measured value is due to the irregular shape and size of filler in nanocomposite as opposed to regular size in the theory as predicted.

3.4. *Friction and wear properties*

Fig. 4a shows the wear with sliding time for pristine PVDF and its nanocomposites with clay. The sliding speed is kept constant at 100 RPM under the normal load of 50 N. Wear decreases with increasing nanoclay content up to 4 wt.%. Similarly, the coefficient of friction, with sliding time, is plotted in Fig. 4b. The coefficient of friction of pristine PVDF is increasing with the sliding time and does not stabilize even after 20 min. In case of nanocomposites (1–4 wt.% nanoclay), the coefficient of friction increases first up to ~5 min followed by its stabilization. The addition of nanoclay stabilizes the coefficient of friction due to the easier transfer layer formation and the stronger adhesive strength in the transfer layer and the counter face upon the addition of nanoclay [32]. However, nanoclay reduces the coefficient of friction of PVDF effectively (~30%). Effect of nanoclay concentration on the friction coefficient, with different loads, is shown in Fig. 4c. Nanoclay concentration of 4 wt.% (PC4) is the most effective one for reducing the friction behaviour under different loads. The lowering of load is related with lower coefficient of friction. At a particular nanoclay concentration, the coefficient of friction decreases as compared to pristine PVDF at a particular applied load. For instance, the coefficient of friction for PC4 decreases by 30, 35 and 33% as compared to pristine PVDF, corresponding to the load of 20, 50 and 100 N, respectively. This result indicates that the nanoclay concentration of 1–4 wt.% is able to improve the wear and friction behaviour of PVDF, while the higher concentration of nanoclay is not so suitable to reduce the friction and wear of the system.

Fig. 4d shows the scanning electron microscope images of worn surfaces of pristine PVDF and its nanocomposites under 50 N load. The surface of pristine PVDF has several deep and wide scraps, which is due to the plastic deformation under wear while the nanocomposite containing 2 and 4 wt.% nanoclay is quite smoother, with limited light scraps. For the nanocomposite containing 8 wt.% nanoclay (Supplementary Fig. S4), the worn surface has lots of scraps, and the worn surface seemed like being exfoliated. This may be due to the high content nanoclay agglomeration (could not combine well with the PVDF matrix). However, the results show that the adding of nanoclay alters the wear properties of PVDF nanocomposites. The nanocomposites show the ability to resist wear, but at high clay concentration, the different behaviour may be due to the phase change and the aggregation of nanoclay.

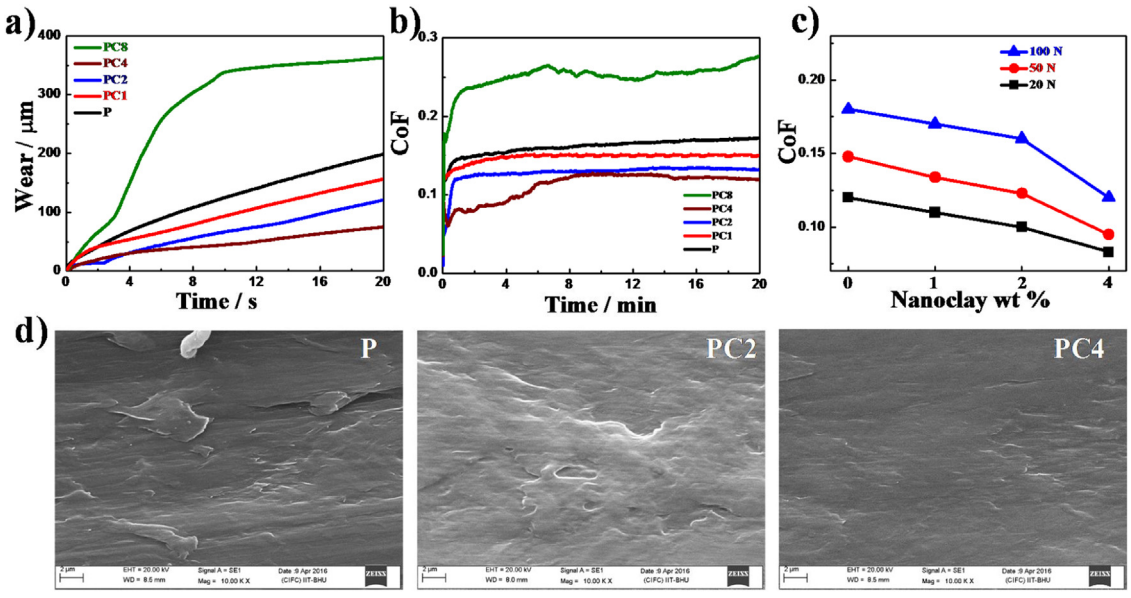

Fig. 4 – (a) Wear behaviour of pristine PVDF and indicated nanocomposites; (b) the coefficient of friction at 50 N load for pristine PVDF and its nanocomposites; (c) the changes in coefficient of friction with nanoclay content at different loading; (d) scanning electron microscopic images for PVDF and nanocomposites after wear experiment.

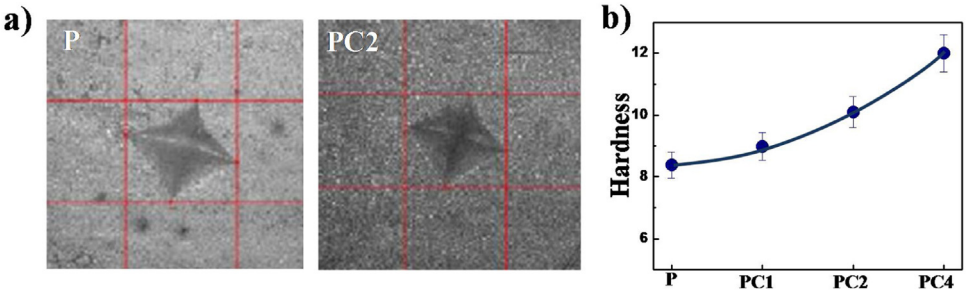

Fig. 5 – (a) Images of indents in Vicker hardness test and (b) corresponding Vickers hardness for pristine PVDF and nanocomposites.

3.5. *Hardness analysis*

Fig. 5a shows the Vickers hardness test results for pristine PVDF and its nanocomposites. Three to four indentations are made to confirm the harness results. The Vickers hardness test calculates the hardness using the equation:

$$HV = 1.854\,L/d^2 \quad (4)$$

where L is the load in kgf and d is the average length of diagonal left by indenter in mm.The hardness of the nanocomposite containing up to 4 wt.% nanoclay increases by 50% with the increasing nanoclay content (Fig. 5b). This is because the reinforcing agent (nanoclay) increases the load carrying capacity of the nanocomposite but at higher nanoclay concentration agglomeration of clay platelets occur, which in turn induces stress concentration and cracking. Mechanical behavior of PVDF nanocomposites has been studied using varied filler content and optimized clay concentration where stiffness and toughness have improved without any trade-off. Wear and hardness also exhibit similar condition and this work demonstrates the suitable conditions for the real applications of PVDF nanocomposites. The improvement in mechanical properties in composite has potential applications in sensor and actuators being piezoelectric in nature in presence of nanoclay.

4. Summary and conclusions

PVDF-clay nanocomposites have been prepared through solution method to study the mechanical and wear behaviour. XRD and FTIR are used to understand the effect on structure on incorporating the nanoclay in PVDF matrix. DSC has been used to analyse the crystallinity of pristine PVDF and the nanocomposites. Uniaxial tensile testing, wear and hardness are used to study the mechanical and frictional behaviour of the nanocomposites at different nanoclay content under various loads. The major findings of the study are the following:

1 After incorporating the nanoclay in PVDF matrix, piezoelectric β and γ-phase are nucleated instead of α-phase in pristine PVDF. The extent of β-phase increases with the enhancement of nanoclay content while the crystallinity decreases.

2 Nanoclay content of 1 to 4 wt.% in the nanocomposites are effective to improve the mechanical and tribological properties. The nanoclay acts as a reinforcing agent and reduces the frictional coefficient. For less wear, the increased polarity caused by the transformation from α to β-phase in the nanocomposite is responsible for low wear in the nanocomposite at lower percentage of loading. Theoretical models perfectly fit the overall improvement in mechanical properties of PVDF nanocomposites.
3 The decrease in mechanical strength of 8 wt.% nanoclay might be due to less uniaxial orientation of nanoclay platelets or the aggregation of clay platelets. Higher clay content nanocomposites show high wear due to weak compatibility between PVDF and nanoclay arising from greater agglomeration.

Conflict of interest

The authors declare no conflict of interest.

Acknowledgement

AG acknowledges the institute for her teaching assistantship.

Appendix A. Supplementary data

Supplementary material related to this article can be found, in the online version, at doi:https://doi.org/10.1016/j.jmrt.2019.09.059.

REFERENCES

[1] Usuki A, Hasegawa N, Kato M, Kobayashi S. Polymer-clay nanocomposites. Inorganic polymeric nanocomposites and membranes. Advances in polymer science, vol 179. Berlin, Heidelberg: Springer; 2005, http://dx.doi.org/10.1007/b104481.
[2] Meng H, Sui GX, Xie GY, Yang R. Friction and wear behavior of carbon nanotubes reinforced polyamide 6 composites under dry sliding and water lubricated condition. Compos Sci Technol 2009;69(5):606–11, http://dx.doi.org/10.1016/J.COMPSCITECH.2008.12.004.
[3] Kawai H. The piezoelectricity of poly(vinylidene fluoride). Jpn J Appl Phys 1969;8(7):975–6, http://dx.doi.org/10.1143/JJAP.8.975.
[4] Lovinger AJ. Ferroelectric polymers. Science (New York, N.Y.) 1983;220(4602):1115–21, http://dx.doi.org/10.1126/science.220.4602.1115.
[5] Peng QY, Cong PH, Liu XJ, Liu TX, Huang S, Li TS. The preparation of PVDF/clay nanocomposites and the investigation of their tribological properties. Wear 2009;266(7–8):713–20, http://dx.doi.org/10.1016/j.wear.2008.08.010.
[6] Xu H, Cheng ZY, Olson D, Mai T, Zhang QM, Kavarnos G. Ferroelectric and electromechanical properties of poly(vinylidene-fluoride-trifluoroethylene-chlorotrifluoroethylene) terpolymer. Appl Phys Lett 2001;78(16):2360–2, http://dx.doi.org/10.1063/1.1358847.
[7] Hammes PCA, Regtien PPL. An integrated infrared sensor using the pyroelectric polymer PVDF. Sens Actuators A Phys 1992;32(1–3):396–402, http://dx.doi.org/10.1016/0924-4247(92)80019-Y.
[8] Liu F, Hashim NA, Liu Y, Abed MRM, Li K. Progress in the production and modification of PVDF membranes. J Membr Sci 2011;375(1–2):1–27, http://dx.doi.org/10.1016/J.MEMSCI.2011.03.014.
[9] Sanchez J-Y, Alloin F, Saunier J. PVDF-based polymers for lithium batteries. Fluorinated Mater Energy Convers 2005:305–33, http://dx.doi.org/10.1016/B978-008044472-7/50042-4.
[10] Kumar C, Gaur A, Rai SK, Maiti P. Piezo devices using poly(vinylidene fluoride)/reduced graphene oxide hybrid for energy harvesting. Nano-Structures Nano-Objects 2017;12:174–81, http://dx.doi.org/10.1016/J.NANOSO.2017.10.006.
[11] Kang SJ, Park YJ, Hwang JY, Jeong HJ, Lee JS, Kim KJ, et al. Localized pressure-induced ferroelectric pattern arrays of semicrystalline poly(vinylidene fluoride) by microimprinting. Adv Mater 2007;19(4):581–6, http://dx.doi.org/10.1002/adma.200601474.
[12] Davis GT, McKinney JE, Broadhurst MG, Roth SC. Electricfieldinduced phase changes in poly(vinylidene fluoride). J Appl Phys 1978;49(10):4998–5002, http://dx.doi.org/10.1063/1.324446.
[13] Electric energy storage properties of poly(vinylidene fluoride). Appl Phys Lett 2010;96(19):192905, http://dx.doi.org/10.1063/1.3428656.
[14] Benz M, Euler WB, Gregory OJ. The role of solution phase water on the deposition of thin films of poly(vinylidene fluoride). Macromolecules 2002;35:2688, http://dx.doi.org/10.1021/MA011744F.
[15] Wang F, Lack A, Xie Z, Frübing P, Taubert A, Gerhard R. Ionic-liquid-induced ferroelectric polarization in poly(vinylidene fluoride) thin films. Appl Phys Lett 2012;100(6):062903, http://dx.doi.org/10.1063/1.3683526.
[16] Buckley J, Cebe P, Cherdack D, Crawford J, Ince BS, Jenkins M, et al. Nanocomposites of poly(vinylidene fluoride) with organically modified silicate. Polymer 2006;47(7):2411–22, http://dx.doi.org/10.1016/j.polymer.2006.02.012.
[17] Ramasundaram S, Yoon S, Kim KJ, Park C. Preferential formation of electroactive crystalline phases in poly(vinylidene fluoride)/organically modified silicate nanocomposites. J Polym Sci B: Polym Phys 2008;46(20):2173–87, http://dx.doi.org/10.1002/polb.21550.
[18] Furukawa T. Ferroelectric properties of vinylidene fluoride copolymers. Phase Transit 1989;18(3–4):143–211, http://dx.doi.org/10.1080/01411598908206863.
[19] Luo Y, Yu W, Xu F. Surface modification and vapor-induced response of poly(vinylidene fluoride)/carbon black composite conductive thin films. Polym Plast Technol Eng 2011;50(11):1084–90.
[20] Liu Q, Tu J, Wang X, Yu W, Zheng W, Zhao Z. Electrical conductivity of carbonnanotube/poly(vinylidene fluoride) composites prepared by high-speed mechanical mixing. Carbon 2012;50(1):339–41, http://dx.doi.org/10.1016/j.carbon.2011.08.051.
[21] Scheinbeim J, Nakafuku C, Newman BA, Pae KD. High-pressure crystallization of poly(vinylidene fluoride). J Appl Phys 1979;50(6):4399–405, http://dx.doi.org/10.1063/1.326429.
[22] Newman BA, Yoon CH, Pae KD, Scheinbeim JI. Piezoelectric activity and fieldinduced crystal structure transitions in poled poly(vinylidene fluoride) films. J Appl Phys 1979;50(10):6095–100, http://dx.doi.org/10.1063/1.325778.
[23] Gaur A, Kumar C, Tiwari S, Maiti P. Efficient energy harvesting using processed poly(vinylidene fluoride) nanogenerator. ACS Appl Energy Mater 2018;1(7):3019–24, http://dx.doi.org/10.1021/acsaem.8b00483.

[24] Gaur A, Kumar C, Shukla R, Maiti P. Induced piezoelectricity in poly(vinylidene fluoride) hybrid as efficient energy harvester. ChemistrySelect 2017;2(27):8278–87, http://dx.doi.org/10.1002/slct.201701780.
[25] Thangavel E, Ramasundaram S, Pitchaimuthu S, Hong SW, Lee SY, Yoo SS, et al. Structural and tribological characteristics of poly(vinylidene fluoride)/functionalized graphene oxide nanocomposite thin films. Compos Sci Technol 2014;90:187–92, http://dx.doi.org/10.1016/j.compscitech.2013.11.007.
[26] Brostow W, Keselman M, Mironi-Harpaz I, Narkis M, Peirce R. Effects of carbon black on tribology of blends of poly(vinylidene fluoride) with irradiated and non-irradiated ultrahigh molecular weight polyethylene. Polymer 2005;46(14):5058–64, http://dx.doi.org/10.1016/J.POLYMER.2005.01.088.
[27] Bismarck A, Schulz E. Adhesion and friction behavior between fluorinated carbon fibers and poly(vinylidene fluoride). J Mater Sci 2003;38(24):4965–72, http://dx.doi.org/10.1023/B:JMSC.0000004420.65554.1e.
[28] Garcia JL, Koelling KW, Seghi RR. Mechanical and wear properties of polymethylmethacrylate and polyvinylidene fluoride blends. Polymer 1998;39(8–9):1559–67, http://dx.doi.org/10.1016/S0032-3861(97)00498-9.
[29] El Achaby M, Arrakhiz FZ, Vaudreuil S, Essassi EM, Qaiss A, Bousmina M. Preparation and characterization of melt-blended graphene nanosheets-poly(vinylidene fluoride) nanocomposites with enhanced properties. J Appl Polym Sci 2013;127(6):4697–707, http://dx.doi.org/10.1002/app.38081.
[30] Moussaif N, Groeninckx G. Nanocomposites based on layered silicate and miscible PVDF/PMMA blends: melt preparation, nanophase morphology and rheological behaviour. Polymer 2003;44(26):7899–906, http://dx.doi.org/10.1016/j.polymer.2003.10.053.
[31] Priya L, Jog JP. Intercalated poly(vinylidene fluoride)/clay nanocomposites: structure and properties. J Polym Sci B: Polym Phys 2003;41(1):31–8, http://dx.doi.org/10.1002/polb.10355.
[32] Jawahar P, Gnanamoorthy R, Balasubramanian M. Tribological behaviour of clay-thermoset polyester nanocomposites. Wear 2006;261(7–8):835–40, http://dx.doi.org/10.1016/j.wear.2006.01.010.
[33] Srinath G, Gnanamoorthy R. Two-body abrasive wear characteristics of nylon clay nanocomposites—effect of grit size, load, and sliding velocity. Mater Sci Eng A 2006;435–436:181–6, http://dx.doi.org/10.1016/J.MSEA.2006.07.117.
[34] Lai CY, Groth A, Gray S, Duke M. Enhanced abrasion resistant PVDF/nanoclay hollow fibre composite membranes for water treatment. J Membr Sci 2014;449:146–57, http://dx.doi.org/10.1016/j.memsci.2013.07.062.
[35] Hasook A, Muramatsu H, Tanoue S, Iemoto Y, Unryu T. Preparation of nanocomposites by melt compounding polylactic acid/polyamide 12/organoclay at different screw rotating speeds using a twin screw extruder. Polym Compos 2008;29(1):1–8, http://dx.doi.org/10.1002/pc.20336.
[36] Sajkiewicz P, Wasiak A, Goclowski Z. Phase transitions during stretching of poly(vinylidene fluoride). Eur Polym J 1999;35(3):423–9, http://dx.doi.org/10.1016/S0014-3057(98)00136-0.
[37] Linares A, Acosta JL. Pyro-piezoelectrics polymers materials—I. Effect of addition of PVA and/or PMMA on overall crystallization kinetics of PVDF from isothermal and non-isothermal data. Eur Polym J 1995;31(7):615–9, http://dx.doi.org/10.1016/0014-3057(95)00020-8.
[38] Pramoda K, Mohamed A, Yee Phang I, Liu T. Crystal transformation and thermomechanical properties of poly(vinylidene fluoride)/clay nanocomposites. Polym Int 2005;54(1):226–32, http://dx.doi.org/10.1002/pi.1692.
[39] Wunderlich B. Macromolecular physics. Crystal nucleation, growth, annealing, vol. 2. Academic Press; 1976.
[40] Shah D, Maiti P, Gunn E, Schmidt DF, Jiang DD, Batt CA, et al. Dramatic enhancements in toughness of polyvinylidene fluoride nanocomposites via nanoclay-directed crystal structure and morphology. Adv Mater 2004;16(14):1173–7, http://dx.doi.org/10.1002/adma.200306355.
[41] Halpin JC, Louis ST, Kardos JL. The Halpin–Tsai equations: a review. Polym Eng Sci 1976;16(5):344–52.
[42] Zhao X, Zhang Q, Chen D, Lu P. Enhanced mechanical properties of graphene-based poly(vinyl alcohol) composites. Macromolecules 2010;43(5):2357–63, http://dx.doi.org/10.1021/ma902862u.
[43] Liang J, Huang Y, Zhang L, Wang Y, Ma Y, Guo T, et al. Molecular-level dispersion of graphene into poly(vinyl alcohol) and effective reinforcement of their nanocomposites. Adv Funct Mater 2009;19(14):2297–302, http://dx.doi.org/10.1002/adfm.200801776.
[44] Mallick PK, Retrieved from https://www.crcpress.com/Fiber-Reinforced-Composites-Materials-Manufacturing-and-Design-Third/Mallick/p/book/9780849342059, 2008.
[45] Qian D, Dickey EC, Andrews R, Rantell T. Load transfer and deformation mechanisms in carbon nanotube-polystyrene composites. Appl Phys Lett 2000;76(20):2868–70, http://dx.doi.org/10.1063/1.126500.